




## Article

# Drought Damage Assessment for Crop Insurance Based on Vegetation Index by Unmanned Aerial Vehicle (UAV) Multispectral Images of Paddy Fields in Indonesia

Yu Iwahashi <sup>1,2</sup>, Gunardi Sigit <sup>3</sup>, Budi Utoyo <sup>3</sup>, Iskandar Lubis <sup>4</sup>, Ahmad Junaedi <sup>4</sup>, Bambang Hendro Trisasongko <sup>4</sup>, I Made Anom Sutrisna Wijaya <sup>5</sup>, Masayasu Maki <sup>6</sup>, Chiharu Hongo <sup>7</sup> and Koki Homma <sup>2,\*</sup>

<sup>1</sup> Graduate School of Agriculture, Kyoto University, Kyoto 6068224, Japan

<sup>2</sup> Graduate School of Agricultural Science, Tohoku University, Sendai 9808572, Japan

<sup>3</sup> Regional Office of Food Crops Service West Java Province, Cianjur 43283, Indonesia

<sup>4</sup> Faculty of Agriculture, IPB University, Bogor 16680, Indonesia

<sup>5</sup> Department of Agricultural and Bio-System Engineering, Udayana University, Badung 803611, Indonesia

<sup>6</sup> Faculty of Food and Agricultural Sciences, Fukushima University, Fukushima 9061296, Japan

<sup>7</sup> Center for Environmental Remote Sensing, Chiba University, Chiba 2638522, Japan

\* Correspondence: koki.homma.d6@tohoku.ac.jp; Tel.: +81-22-757-4083; Fax: +81-22-757-4085

**Abstract:** Drought is increasingly threatening smallholder farmers in Southeast Asia. The crop insurance system is one of the promising countermeasures that was implemented in Indonesia in 2015. Because the damage assessment in the present system is conducted through direct investigations based on appearance, it is not objective and needs a long time to cover large areas. In this study, we investigated a rapid assessment method for paddy fields using a vegetation index (VI) taken by an unmanned aerial vehicle (UAV) with a multispectral camera in 2019 and 2021. Then, two ways of assessment for drought damage were tested: linear regression (LR) based on a visually assessed drought level (DL), and k-means clustering without an assessed DL. As a result, EVI2 could represent the damage level, showing the tendency of the decrease in the value along with the increasing DL. The estimated DL by both methods mostly coincided with the assessed DL, but the concordance rates varied depending on the locations and the number of assessed fields. Differences in the growth stage and rice cultivars also affected the results. This study revealed the feasibility of the UAV-based rapid and objective assessment method. Further data collection and analysis would be required for implementation in the future.

**Keywords:** crop insurance; drought; Indonesia; rice; unmanned aerial vehicle; vegetation index



**Citation:** Iwahashi, Y.; Sigit, G.; Utoyo, B.; Lubis, I.; Junaedi, A.; Trisasongko, B.H.; Wijaya, I.M.A.S.; Maki, M.; Hongo, C.; Homma, K. Drought Damage Assessment for Crop Insurance Based on Vegetation Index by Unmanned Aerial Vehicle (UAV) Multispectral Images of Paddy Fields in Indonesia. *Agriculture* **2023**, *13*, 113. <https://doi.org/10.3390/agriculture13010113>

Academic Editor: Jiyu Li

Received: 23 October 2022

Revised: 26 December 2022

Accepted: 27 December 2022

Published: 30 December 2022



**Copyright:** © 2022 by the authors. Licensee MDPI, Basel, Switzerland. This article is an open access article distributed under the terms and conditions of the Creative Commons Attribution (CC BY) license (<https://creativecommons.org/licenses/by/4.0/>).

## 1. Introduction

Rice is the main staple crop in Indonesia, where 546 million tons of rice were produced in 2020, making it the fourth highest rice-producing country in the world [1]. The inflation of production has been attributed to various aspects such as high-yielding modern cultivars, the use of chemical fertilizers, and mechanization. Furthermore, irrigation water has had a major impact on rice production, especially during the dry season. The Indonesian government has continuously promoted the construction of irrigation networks, which were partly established during the Dutch colonization era [2]. However, only 0.38% of agricultural land in the country is equipped with irrigation facilities [3]; therefore, most paddy fields are rainfed with unstable water conditions, some of which are prone to cause drought [4]. The recent prolonged drought in 2015 resulted in the loss of almost 600 kilotons of paddy production in Indonesia [5]. In addition, climate change has caused more drought events with longer dry seasons and indeterminate rainfall patterns, which could be harmful, especially to small-scale or family farmers, by causing losses or failures of rice crops [6].

For smallholder farmers, crop insurance is a promising countermeasure against climate variability. It compensates for harvest losses due to biotic and abiotic stresses such as pests, diseases, floods, and drought, and ensures that farmers have a minimum working capital for the next planting season [7]. Mahul and Stutley (2010) estimated that 104 countries had some form of insurance in 2008 and that the total premium collected that year, including premium subsidies, was USD 20 billion [8]. Agricultural insurance can be broadly classified into two types based on the ways of determining insurance payment: index-based and indemnity-based [9]. Index-based insurance determines the payment based on indices of climatic components affecting crop yield such as the amount of precipitation. Indemnity-based insurance determines the payment based on damage or yield affected by various types of stress. Index-based insurance has the advantages of easy and objective assessment, and being free from moral hazards whereby farmers cease to manage sufficiently in order to gain money [9]. Indemnity-based insurance enables insured farmers to obtain an insurance payment for the damage level of each field but requires much greater time and labor for assessment.

In Indonesia, agricultural insurance for rice was implemented by the national government in 2015. The insurance payment was equal to the cost of production (i.e., agricultural production cost insurance, APCI) [10]. The criterion of the insurance payment was set to 75%, which means that farmers receive insurance if they obtain an assessment result that shows more than 75% of their farmland has been destroyed by disaster (e.g., drought). Because the assessment has to be conducted by investigators observing each field, it takes time to assess all paddy fields in large areas. Farmers have to leave the field unharvested and wait until the assessment is finished. This means that they cannot harvest the rest of the fields even if they are not damaged, which may decrease the rice quality. The number of investigators becomes a constraint on the rapid assessment. Fairness is another limitation of the insurance because the damage is assessed based on their observations.

Recently, remote sensing technology has made significant advances in agricultural monitoring. Remote sensing is a multiscale technology that encompasses a ground level measurement, UAV-based measurement, and satellite sensing. For example, at the satellite scale sensing, the transplanting date was estimated using Sentinel-1 imagery [11], and long-term changes in rice production were quantified using MODIS LAI (leaf area index) data [12]. Most remote sensing techniques are based on crop or soil reflectance of radiation, and multispectral reflectance can deliver information on subjects. The vegetation index (VI), which is usually calculated from two spectral band reflectance, has been developed to monitor crop growth or status such as the above ground biomass [13], leaf area index [14], or chlorophyll content [15]. Though satellite-based VI can detect changes in crop production or land use in large areas [16,17], spatial and temporal resolution are often constraints in field-scale measurement. Recently, unmanned aerial vehicle (UAV)-based VI has been utilized in field-scale measurements, such as the estimation of leaf area index [14] or crop damage assessment [18]. UAV-based VI has been investigated in high-throughput phenotyping of drought tolerance in various plants such as forage grasses [19], wheat [20], and tomato [21]. Water stress induces stomatal closure, resulting in increased surface temperature of the leaf in the short term. The decline in photosynthesis and degradation of chlorophyll turn leaves yellow in the long term. At the same time, drought can cause temporary or enduring wilting of leaves and restrict leaf growth. Leaf color change or relative decrease in leaf area would be visible indicators of drought damage and probably reflected in VI. UAV-based VI would apply to the field-based assessment of drought damage. However, few studies have focused on the investigation of farmers managing fields to test the feasibility of the UAV-based VI on drought damage assessment.

In this study, UAV-based vegetation indices (VIs) were analyzed to investigate an alternative method to the current visual assessment of drought damage. First, we compared several vegetation indices in terms of correspondence to the visual assessment by investigators. Second, VI-based assessment methods were explored and evaluated. Finally, feasibility regarding reliability and convenience was discussed.

## 2. Materials and Methods

### 2.1. Study Site

The study site was Cianjur Regency, West Java Province, Indonesia (Figure 1). West Java Province has the highest rice production in Indonesia. Cianjur Regency is one of the rice-producing areas in the province, with a large irrigation area (Cihea irrigation area). Rice can be cultivated two or three times a year in the area [11]. Field investigations were conducted three times during the dry season: in August (the first survey) and October (the second survey) 2019, and August 2021 (the third survey) (Table 1). In 2019, Indonesia experienced a prolonged dry season until the end of the year [22]. Each time, three or four locations where paddy fields were affected by drought to some extent were investigated. There were irrigation canals or rivers around the fields, but drought damage was observed because the water was not enough.

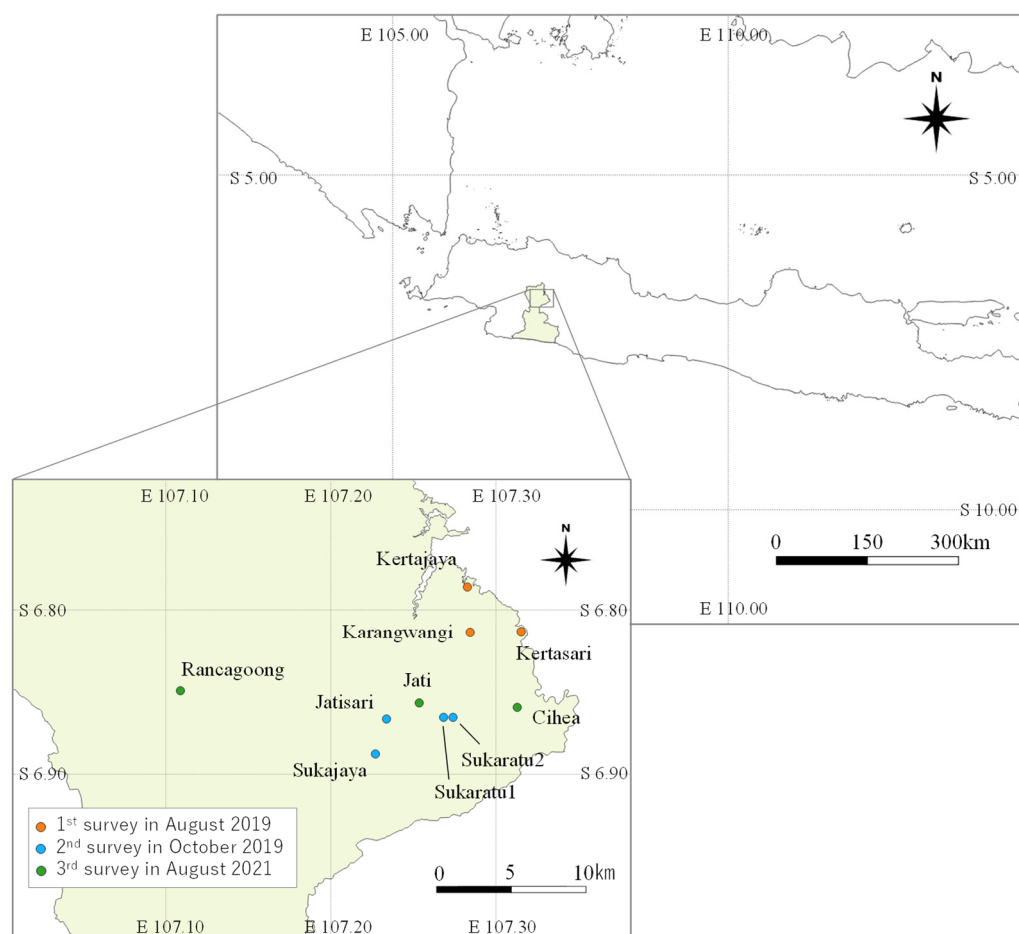


**Figure 1.** Map of the investigation site. The location names are indicated in the lower left map.

### 2.2. Drought Assessment and Field Investigation

As part of their duties, pest observers (POs) belonging to the Regional Office of Food Crops Service, West Java Province, assessed the drought level. The assessment followed the criterion that classified the drought level into four classes depending on the appearance of the rice: drought level (DL) 1 was slight damage, DL4 was failure of the cultivation or no harvest, and DL2 and 3 were between the two classes (Table 2, Figure 2). In the first and second survey in August and October 2019, respectively, DL1-4 were assessed following the criterion. In the third survey in August 2021, DL0 was added to distinguish no drought damage according to our recommendation. In the second survey, the days after planting (DAT) of each location were identified through interviews with farmers.

Information on cultivars as well as the DAT of each assessed field was gathered in the third survey (Table 3).

**Table 1.** Information on each location and assessments by PO.

Survey Date (Growth Stage or DAT)	Name of Location	Number of Assessed and Unassessed (UA) Fields						Total Area * (m <sup>2</sup> )
		DL0	DL1	DL2	DL3	DL4	UA	
1st survey on 7–9 August 2019 (heading to harvesting)	Kertajaya	-	0	6	0	4	14	6312
	Kertasari	-	2	6	0	3	70	17,414
	Karangwangi	-	3	3	4	0	56	16,331
2nd survey on 9–10 October 2019 (DAT 14–60)	Sukajaya	-	3	2	1	0	47	18,470
	Jatisari	-	3	3	0	0	57	22,825
	Sukaratu1	-	0	8	0	0	20	11,399
	Sukaratu2	-	3	0	10	0	58	21,284
3rd survey on 8–9 August 2021 (DAT 45–90)	Ciheia	4	0	5	4	4	66	18,905
	Jati	5	5	5	5	0	21	19,785
	Rancagoong	5	4	1	0	0	14	10,209

\* Total areas of each location were calculated by a sum of polygon areas covering assessed and unassessed fields using QGIS.

**Table 2.** Definition of the drought level (DL) assessment.

Drought Level (DL)	Ratio of Damaged Area	Symptoms
DL0	0%	No obvious symptoms
DL1	25%<	Slight leaf rolling
DL2	25–50%<	Leaf top rolling and yellow
DL3	50–85%<	Almost wilting and yellow leaves
DL4	≥85%	All died or no harvest

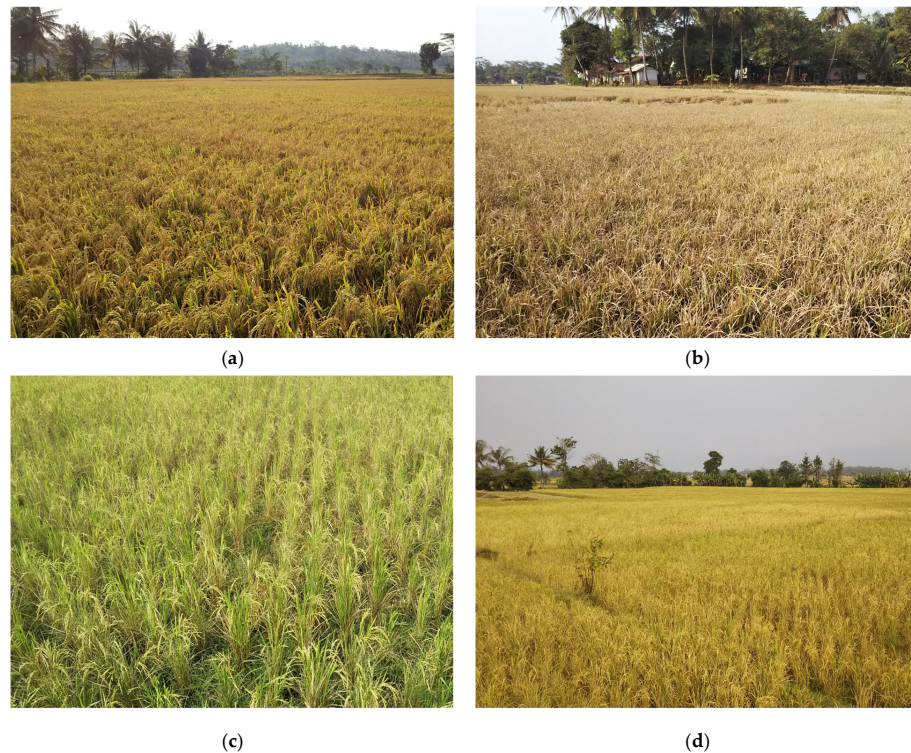


**Figure 2.** Example pictures of assessed fields by a pest observer: (a) paddy fields assessed as DL2 in Kertajaya; (b) assessed as DL4 in Kertajaya; (c) assessed as DL2 in Karangwangi; (d) assessed as DL3 in Karangwangi.

**Table 3.** Details of information on the third survey in 2021.

Location Name	Cultivar	DAT	Number of Assessed Fields	DL
Cihea	Shintanur	79	3	2
	Ciherang	69	4	2/3
	Segon Salak	64/74	7	0/4
	Inpari 32	64/90	3	0/3
Jati	Inpari 32	35	20	0/1/2/3
Rancagoong	Inpari 32	45/60/65/75	9	0/1/2
	Shintanur	65	1	1

We recorded GPS coordinates at four corners of each assessed field using GPS hand receiver eTrex20x (Garmin International Inc., Olathe, KS, USA). Multispectral images were taken with a UAV to cover the investigated locations. The multispectral camera used in 2019 was Sequoia (Parrot SA, Paris, France), which was installed on the UAVs, Mavic Pro (SZ DJI Technology Co., Ltd., Shenzhen, China), and Bluegrass Fields (Parrot SA, Paris, France) in the first and second survey, respectively. The multispectral camera used in the third survey in 2021 was the attachment of UAV, P4 Multispectral (SZ DJI Technology Co., Ltd., Shenzhen, China). The flights of the UAVs were set to cover the directly assessed and unassessed fields with Pix4D capture (Pix4D SA, Prilly, Switzerland) and GS Pro (SZ DJI Technology Co., Ltd., Shenzhen, China) in the first and second surveys in 2019, and the third survey in 2021, respectively. The images were taken at time intervals and other settings were listed in Table 4. The total area and the number of assessed and unassessed fields included in the captured images were listed in Table 1.

**Table 4.** Flight settings of each survey.

	UAV	Camera	Flight Height (m)	Front-Side Overlapping (%)
1st survey	Mavic Pro	Sequoia	50	85–85
2nd survey	Bluegrass	Sequoia	74	85–85
3rd survey	P4 Multispectral	P4 Multispectral	50	85–75

### 2.3. Data Processing

UAV pictures taken at each location were composited into ortho-mosaic images using Pix4D mapper software (Pix4D SA, Prilly, Switzerland). The ortho-mosaic images contain GPS information for every pixel, supporting analysis in Geographic Information System (GIS): Quantum GIS software (QGIS ver. 3.1.6). Each assessed field by POs was identified in the images by the recorded GPS coordinates and hand-drawn field maps. Although the GPS coordinates were not completely consistent with the images, the hand-drawn maps helped to recognize the assessed fields in the images. For the sequoia in the first and second survey, the reflectance of each spectral band, green (G), red (R), and near-infrared (NIR) was obtained by calibrating with the standard reflectance board, Calibrated Reflectance Panel (MicaSense, Seattle, DC, USA) and Sequoia calibration target (Parrot SA, Paris, France), respectively. The reflectance factor (reflected radiation divided by incident radiation for the spectral band) for each spectral band was used in the analysis of the third survey because the multispectral camera of P4 Multispectral was not considered to use a standard reflectance board.

The first step was obtaining ortho-mosaic images of VIs, which were the green–red ratio vegetation index (GRRI) [23], green–red vegetation index (GRVI) [24], normalized difference vegetation index (NDVI) [25], green normalized difference vegetation index (GNDVI) [26], and enhanced vegetation index (EVI2) [27]. The calculating formulas are listed in Table 5. The first two VIs use the reflectance of green and red wavelengths, mainly indicating leaf color. The others use near-infrared band, which probably represents

green leaves coverage. The next step was drawing polygons covering each assessed and unassessed paddy field in the images (Figure 3). The third step was obtaining the average and 1 to 99 percentiles of VIs for each field.

**Table 5.** Calculation formulas for five vegetation indices: [G], [R], [NIR] are reflectance of each band.

Vegetation Index	Calculation Formula	
GRI	$GRI = [G]/[R]$	[23]
GRVI	$GRVI = ([G] - [R])/([G] + [R])$	[24]
NDVI	$NDVI = ([NIR] - [R])/([NIR] + [R])$	[17]
GNDVI	$GNDVI = ([NIR] - [G])/([NIR] + [G])$	[19]
EVI2	$EVI2 = G * ([NIR] - [R])/([NIR] + C * [R] + L)$ (G = 2.5, C = 2.4, L = 1)	[20]

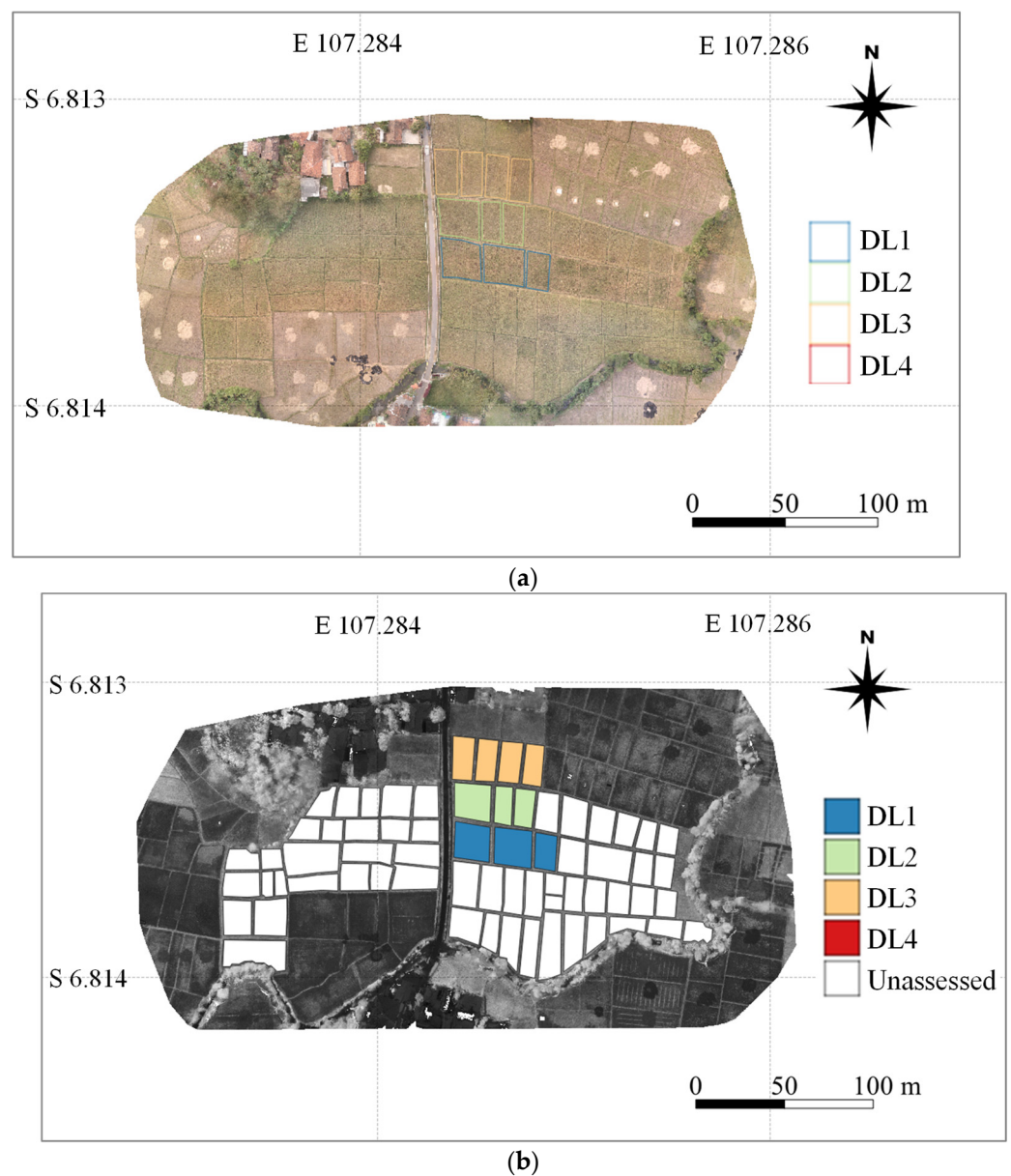


**Figure 3.** Examples of polygons for assessed and unassessed paddy fields in Karangwangi: (a) assessed fields are indicated in an ortho-mosaic image of RGB; (b) assessed and unassessed fields are shown in a calculated EVI2 image from multispectral image.

#### 2.4. Evaluating Methods

Linear regression analysis was applied to compare VIs based on the relation between the average VI and DL for the data obtained in the first and second surveys, respectively. After we selected EVI2 to evaluate DL based on the regression analysis, two assessment methods were tested for the investigated locations (Figure 4): one method used linear regression (LR) of DL against the average EVI2 (method1); the other method utilized k-means clustering, which classified paddy fields based on similarities of 1 to 99 percentiles of EVI2 for each field (method2). Method2 does not need on-site assessments of DL but needs the least and the most DL to decide the number of classes. For this time, the number was set to the same as the result of method1. In Sukaratu1, the regression equation was not obtained since the eight fields were assessed only as DL2; therefore, it was calculated exceptionally: the least, median, and highest values of EVI2 in the eight fields were used as DL1.5, DL2, and DL2.5, respectively. As for method2, extraction of 1–99 percentiles and k-means clustering was performed for each location using R (version 4.0.1 and 4.1.2) and R Studio Software (R Studio, PBC).

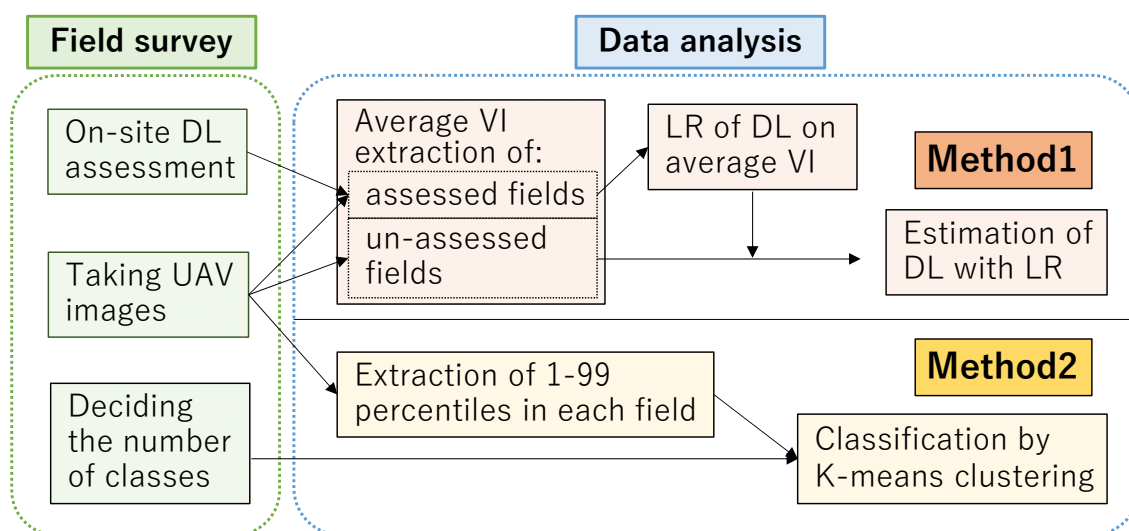


**Figure 4.** Flow chart of two methods for drought damage assessment.

### 3. Results

The relations between the DL assessed by POs and the average VI of the corresponding field are shown in Figure 5. Although the relationship was significantly different among the investigated locations, a common tendency was observed that all VI values decreased as DL increased. The slopes of the regression equation between the three locations were similar in EVI2 (Figure 5e). The similar relationship was indicated in the result of the second survey except Jatisari where all VIs were significantly low. In Jatisari, the rice crop was only in its second week after transplanting. In most of the locations, VI values of DL2 showed large variations, and those of DL3 and DL4 were either similar, or higher in DL4 than in DL3, in the case of Kertasari (Figure 5). The average determination coefficients of LR exceeded 0.80 though the number of assessed fields was limited (Table 6). The average determination coefficients in the vegetative stage (obtained in the second survey in October 2019) exceeded 0.90 in GRVI, GRRI, and NDVI, and were relatively higher than those in the heading to harvesting stage (obtained in the first survey in August 2019). Among the five VIs, EVI2 showed the most stable and optimal performance, followed by NDVI. As a result, EVI2 was selected for further analysis.

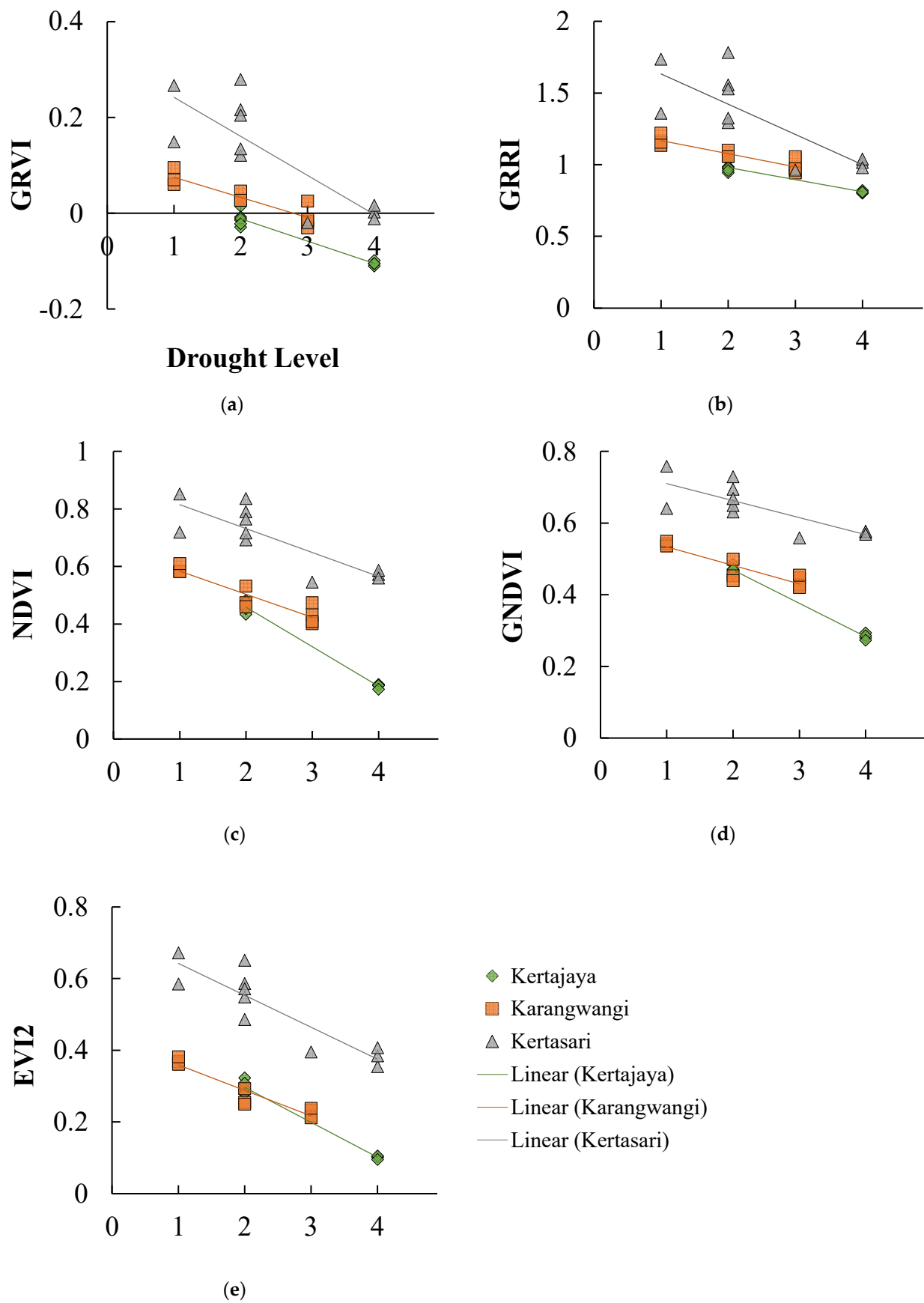


**Figure 5.** The linear relationships between vegetation index and drought level assessed by a pest observer in the 1st survey. (a) GRVI; (b) GRR; (c) NDVI; (d) GNDVI; (e) EVI2.



**Table 6.** Average determination coefficients of linear regression for DL against each VI for investigated locations.

	Average R <sup>2</sup> Value	
	1st Survey	2nd Survey
GRVI	0.81	0.93
GRR1	0.80	0.93
NDVI	0.85	0.92
GNDVI	0.81	0.83
EVI2	0.89	0.89

The concordance rates of classification between the two tested methods and the DL assessed by POs are listed in Table 7. Method1 was not applicable in Cihea since the regression line of the DL on EVI2 was not obtained, probably affecting the low concordance rate for method2. Method1 was generally superior to method2 in terms of the concordance rate, but estimation results from method1 (linear regression) did not exactly coincide with the assessed DL by PO. Classification results using k-means clustering (method2) based on 1–99 percentiles of EVI2 are shown in Figure 6. Each field was clearly classified depending on the similarity of EVI2. However, in Karangwangi, the DL1 and DL2 fields assessed by POs (indicated by diamonds on the lines in Figure 6) were classified into DL2 and DL3, respectively (Figure 6a). As a result, the difference in concordance rates between the two methods was large: the rate of method1 was 100%, while that of method2 was 40% in Karangwangi. In Sukajaya, most assessed fields were classified into the same DL as assessed by POs (Figure 6b), while many of the assessed DLs were different from the classification results in Jati (Figure 6c). The same DL fields assessed by POs indicated the variations in EVI2 in Jati, e.g., seven fields assessed as DL1 by POs showed a large value difference and were classified into DL0 to DL3 by method2 (Figure 6c). On the other hand, the concordance rates of method2 in Kertasari, Sukaratu2, and Rancagoong were higher than those of method1. In Kertajaya, Sukajaya, Jatisari, and Sukaratu2, the concordance rates between the DL assessed by POs and the estimated DL by both methods were higher than 75% (Table 7 and Figure 7). In all locations except for Karangwangi and Cihea, the DLs estimated by method1 and method2 mostly matched each other (Table 7). In Karangwangi, most unassessed fields were estimated to be DL1 by method1, while they were more severely estimated, as DL2 or DL3, by method2 (Figures 6a and 8).

**Table 7.** Concordance rates between assessed DL and estimated DL for method1 and 2 and match rates of all estimated DLs between the two methods.

	Location Name	Concordance Rate (%)		Match Rate (%)
		Method1	Method2	
1st survey	Kertajaya	100	90.0	75.0
	Kertasari	54.5	63.6	74.1
	Karangwangi	100	40.0	47.0
2nd survey	Sukajaya	83.3	83.3	92.5
	Jatisari	100	83.3	71.4
	Sukaratu1	87.5	62.5	71.4
	Sukaratu2	76.9	100	71.8
3rd survey	Cihea	-	17.7	-
	Jati	50.0	35.0	73.2
	Rancagoong	80.0	90.0	91.7
	Total	76.6	62.8	67.9

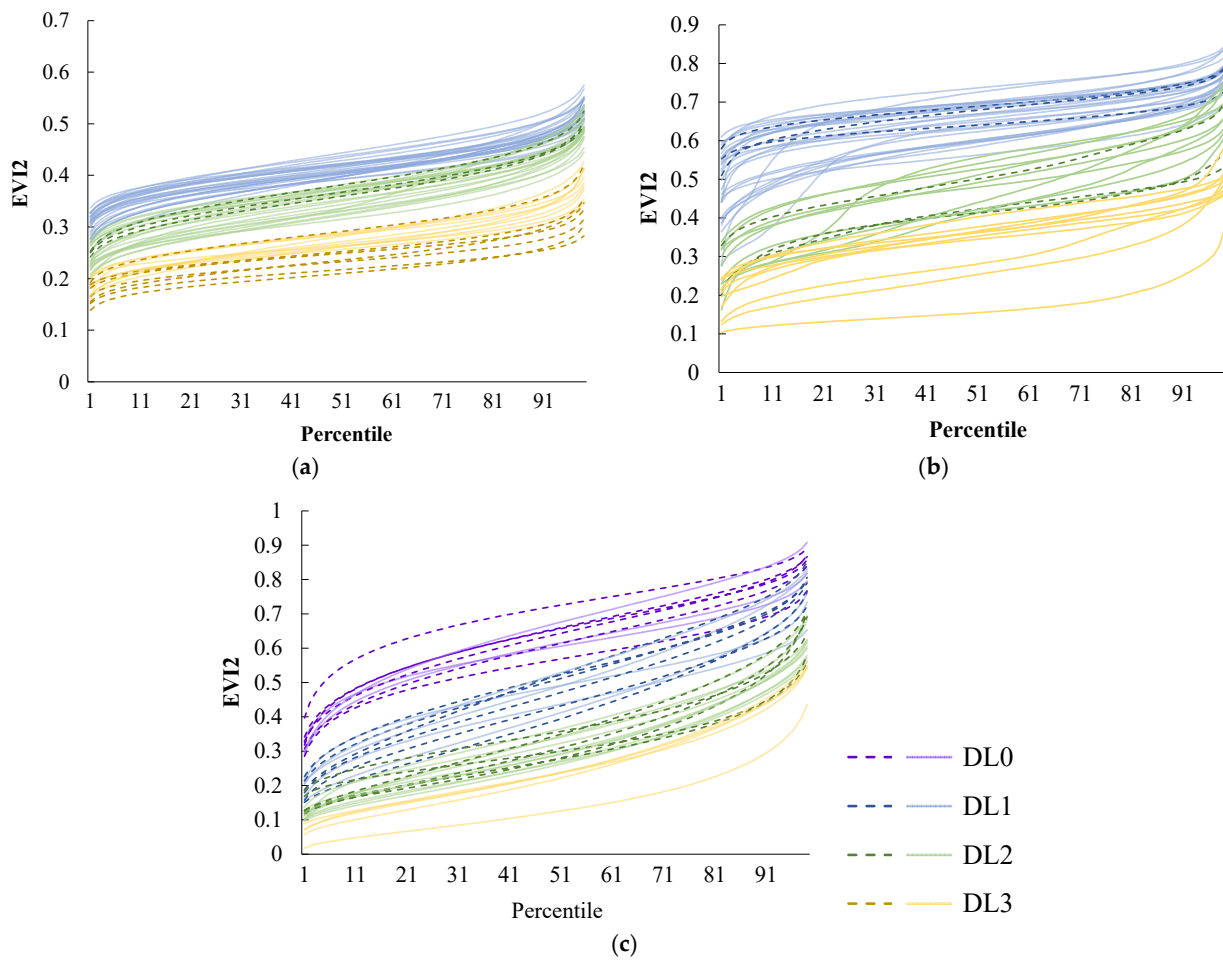


**Figure 6.** EVI2 of 1–99 percentiles for each field: (a) Karangwangi (the first survey); (b) Sukajaya (the second survey); (c) Jati (the third survey). Different colored lines indicate different DLs classified by method2 (k-means clustering). Dotted lines indicate assessed fields by POs with the colors of classified DLs.

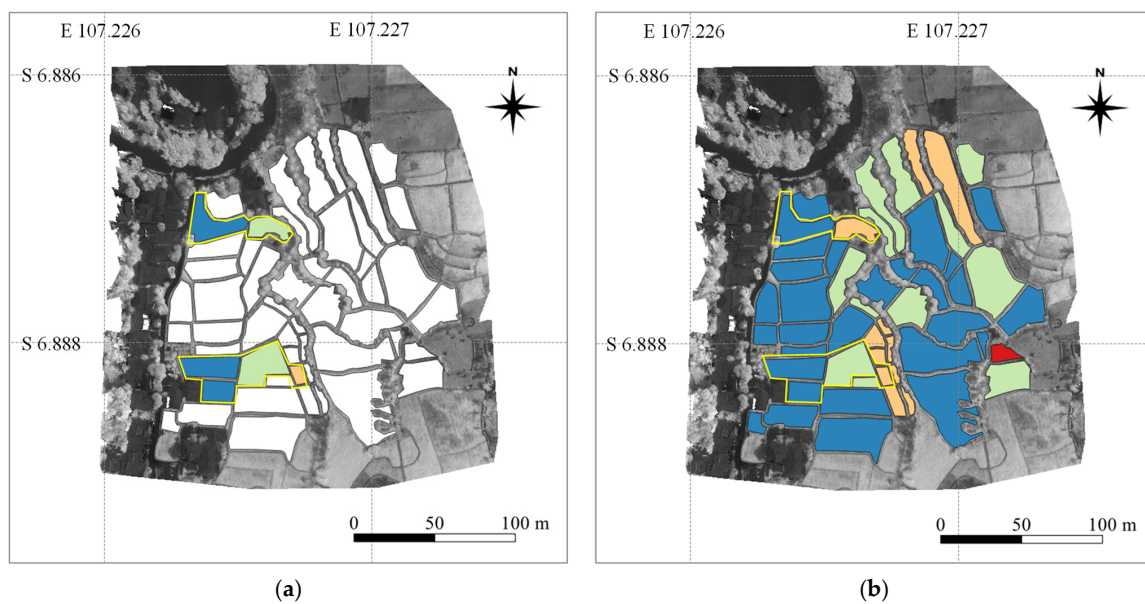
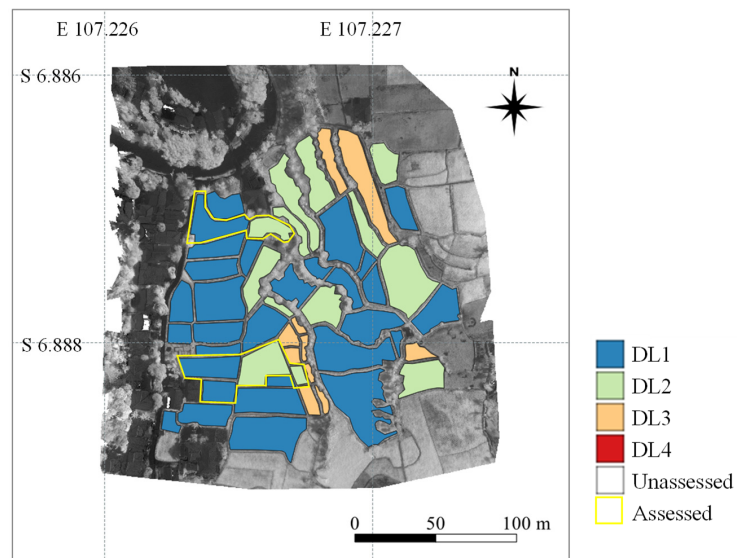
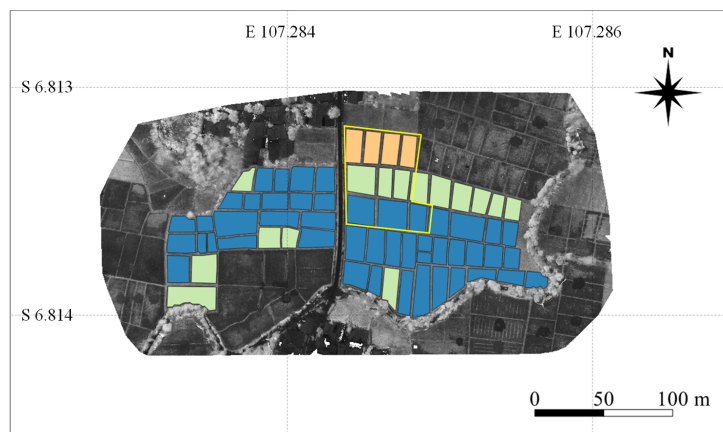


**Figure 7.** Cont.

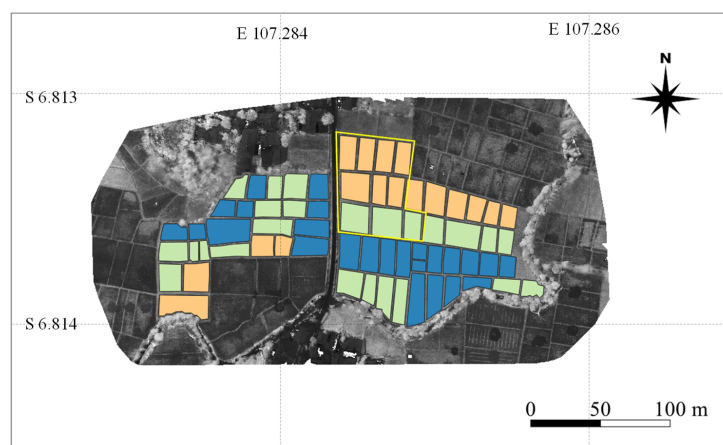


(c)

**Figure 7.** Assessment by a PO and classification results of the two methods in Sukajaya: (a) assessed fields by a PO; (b) an assessment result by method1; (c) an assessment result by method2. Different polygon colors indicate different assessed/classified DLs.



(a)



(b)

**Figure 8.** Classification results of the two methods in Karangwangi: (a) an assessment result by method1; (b) an assessment result by method2. Assessment result by a PO is shown in Figure 3b. Legends are same as Figure 7.

#### 4. Discussion

DL was visually assessed by POs based on differences from non-damaged plants in terms of leaf area and greenness. In this study, VIs derived from UAV images were generally consistent with the DLs by POs for the investigated locations. Since positive correlations were reported between these VIs and plant leaf area or the amount of chlorophyll [28,29], the rice growth condition inhibited by drought was probably reflected in them. In other words, VIs could be an indicator of the DL. In comparing five VIs, those with near-infrared (NIR) band reflectance represented relatively better concordance rates with DLs after the heading stage, while other VIs using red and green band reflectance performed well in the vegetative stage. NIR band reflectance used in various VIs (e.g., NDVI) has often been used to evaluate crop growth and damaged status [13,18]. In this study, EVI2 performed the best in estimating DLs in the first survey. At the harvesting stage, differences in leaf color between damaged and undamaged crops might be small, but EVI2 estimated the LAI difference better than other VIs as Maki et al. (2016) previously reported [28]. The performances in GRVI and GRRI, which do not use NIR band reflectance, were better in the second survey, which may reflect the visible leaf color difference between damaged and undamaged crops. Although the data in this study were still limited to confirm the selection, we selected EVI2 for further analysis as the most stable VI in the performance at both stages. Determination coefficients were generally higher in the second survey than those in the first survey because the differences in appearance between damaged and undamaged crops seemed more visible in leaf area or leaf color in the vegetative stage. The results suggest that the difference in leaf area is the key indicator for determining DL especially after the heading stage. The estimation of DL mainly based on leaf area might cause the difference in regression lines among the investigated locations because leaf area in the non-damaged field differed for each growth stage and cultivar. Accordingly, the estimation should be temporarily conducted at a locational scale, where few cultivars and fewer variations in DAT are expected. At this point, the correlation between DL and EVI2 could not be obtained in Cihea since several cultivars and differences in DAT were observed. Possibly for the same reason, the estimation resulted in lower concordance rates in Kertasari, where paddy fields included rice plants ranging from vegetative to heading stages. If the number of assessments increased in terms of growth stages and cultivars, a general regression would be obtained. The huge number of data points collected will enable us to utilize machine learning methods to estimate DLs in the future.

In previous research [18], damage assessment using VI was conducted by calculating the difference in VI between healthy plants and damaged plants. In this study, we tried to evaluate the unassessed fields using two other methods, linear regression (method1) and k-means clustering (method2), because undamaged paddy fields (assessed as DL0 in this study) were not always available in each location. It was reasonable that method1 resulted in better concordance rates with DLs by POs than method2 since the regression was calculated based on DLs by POs. However, method2 generally recorded more than 60% concordance rates and objectively classified fields based on similarities of 1–99 percentiles of EVI2. The obtained results suggest that both method1 and 2 have the potential to become an alternative method to the present assessment by PO. Method1 is more consistent with the present assessment but needs on-site investigation for several fields to obtain a regression equation. Method2 needs on-site investigation only to obtain the lowest and highest DLs to determine the number of classes for k-means clustering. The selection of the optimal method should be performed by comparing the consistency with the present assessment and the cost of on-site investigation.

The drought assessment method proposed in this study took less time and was less labor-consuming because taking multispectral images with a UAV takes approximately ten to twenty minutes for several hectares. POs can cover larger areas in a day using a UAV. We prepared a manual to disseminate the methods to POs, enabling them to learn the techniques relatively easily. The multispectral images and analysis based on VIs also provide continuous records of damaged fields and objective assessments, both of

which the present visual assessment lacked. The records and objective assessments would substantially improve the insurance system in Indonesia in the future. The preparation of polygons corresponding to each paddy field may be one of the major constraints in the implementation of this method due to its laborious work. However, the polygon data could be utilized repeatedly for various purposes once they were prepared (e.g., GIS-based register and linked information for farmers and their paddy fields). Recently, remote sensing technologies such as satellite-based data have been utilized to generate polygons for each paddy field [30], suggesting the possibility of its automation in the future.

## 5. Conclusions

In Indonesia, a rapid and objective method is required for the crop insurance system. This study investigated a drought damage assessment method for paddy fields using a UAV-based vegetation index during the dry season in 2019 and 2021. VIs decreased when the DL assessed by a PO increased, representing the severity of drought damage. Among five VIs compared in this study, EVI2 showed the most stable performance to estimate DLs. DL estimation by LR based on average EVI2 was mostly consistent with assessed DLs by POs. The large variations in EVI2 even in the same DL fields require several assessed fields to obtain a convincing LR. On the other hand, since k-means clustering without an assessed DL was based on the EVI2, more objective assessment was provided. However, the acceptability of farmers should be investigated further. This study revealed that UAV-based VI was indicated to have substantial feasibility for an agricultural insurance system through the investigation of farmers' fields. Multispectral images captured using UAV can provide continuous records and objective assessments with less time and labor, although acceptability among stakeholders including farmers, investigators, and insurance institutes should be investigated further.

**Author Contributions:** Conceptualization, K.H. and C.H.; methodology, M.M.; formal analysis, Y.I.; investigation, Y.I. and G.S.; writing—original draft, Y.I. and K.H.; writing—review and editing, K.H.; supervision, K.H.; project administration, G.S. and B.U.; funding acquisition, C.H.; validation, G.S., B.U., I.L., A.J., B.H.T. and I.M.A.S.W. All authors have read and agreed to the published version of the manuscript.

**Funding:** This research was funded by JST SATREPS, grant number JPMJSA 1604.

**Institutional Review Board Statement:** Not applicable.

**Informed Consent Statement:** Not applicable.

**Data Availability Statement:** The data presented in this study are available on request from the corresponding author.

**Acknowledgments:** We are grateful to pest observers for assessing drought level and helping field investigations in 2019. Additionally, we appreciate their cooperation in collecting the data in 2021.

**Conflicts of Interest:** The authors declare no conflict of interest.

## References

1. FAOSTAT. Available online: <https://www.fao.org/faostat/en/#data> (accessed on 11 April 2022).
2. Ravesteijn, W. Dutch Engineering Overseas: The Creation of a Modern Irrigation System in Colonial Java. *Knowl. Technol. Policy* **2002**, *14*, 126–144. [CrossRef]
3. Panuju, D.R.; Mizuno, K.; Trisasongko, B.H. The dynamics of rice production in Indonesia 1961–2009. *J. Saudi Soc. Agric. Sci.* **2013**, *12*, 27–37. [CrossRef]
4. Hairmansis, A.; Rumanti, I.A.; Nugraha, Y.; Kato, Y.; Jamil, A. Reaping gains with less rain: Best management practices for drought-prone rice areas in Indonesia. In *Climate-Ready Technologies: Combating Poverty by Raising Productivity in Rainfed Rice Environments in Asia*; Manzanilla, D., Singh, R.K., Kato, Y., Johnson, D., Eds.; International Rice Research Institute: Los Baños, Philippines, 2016; pp. 17–28.
5. Surmaini, E.; Susanti, E.; Syahputra, M.R.; Hadi, T.W. Exploring Standardized Precipitation Index for predicting drought on rice paddies in Indonesia. *IOP Conf. Ser. Earth Environ. Sci.* **2019**, *303*, 012027. [CrossRef]

6. Naylor, R.L.; Battisti, D.S.; Vimont, D.J.; Falcon, W.P.; Burke, M.B. Assessing risks of climate variability and climate change for Indonesian rice agriculture. *Proc. Natl. Acad. Sci. USA* **2007**, *104*, 7752–7757. [[CrossRef](#)] [[PubMed](#)]
7. Pasaribu, S.M. Developing rice farm insurance in Indonesia. *Agric. Agric. Sci. Procedia* **2010**, *1*, 33–41. [[CrossRef](#)]
8. Mahul, O.; Stutley, C.J. *Government Support to Agricultural Insurance*; The World Bank: Washington, DC, USA, 2010; pp. 6–15.
9. The World Bank. Agricultural insurance: A background. In *Weather Index Insurance for Agriculture: Guidance for Development Practitioners*; The World Bank: Washington, DC, USA, 2011; pp. 9–13.
10. Mutaqin, D.J.; Usami, K. Smallholder Farmers' Willingness to Pay for Agricultural Production Cost Insurance in Rural West Java, Indonesia: A Contingent Valuation Method (CVM) Approach. *Risks* **2019**, *7*, 69. [[CrossRef](#)]
11. Manago, N.; Hongo, C.; Sofue, Y.; Sigit, G.; Utoyo, B. Transplanting Date Estimation Using Sentinel-1 Satellite Data for Paddy Rice Damage Assessment in Indonesia. *Agriculture* **2020**, *10*, 625. [[CrossRef](#)]
12. Iwahashi, Y.; Ye, R.; Kobayashi, S.; Yagura, K.; Hor, S.; Soben, K.; Homma, K. Quantification of Changes in Rice Production for 2003–2019 with MODIS LAI Data in Pursat Province, Cambodia. *Remote Sens.* **2021**, *13*, 1971. [[CrossRef](#)]
13. Kross, A.; McNairn, H.; Lapen, D.; Sunohara, M.; Champagne, C. Assessment of RapidEye vegetation indices for estimation of leaf area index and biomass in corn and soybean crops. *Int. J. Appl. Earth Obs. Geoinf.* **2015**, *34*, 235–248. [[CrossRef](#)]
14. Yamaguchi, T.; Tanaka, Y.; Imachi, Y.; Yamashita, M.; Katsura, K. Feasibility of Combining Deep Learning and RGB Images Obtained by Unmanned Aerial Vehicle for Leaf Area Index Estimation in Rice. *Remote Sens.* **2021**, *13*, 84. [[CrossRef](#)]
15. Qiao, L.; Tang, W.; Gao, D.; Zhao, R.; An, L.; Li, M.; Sun, H.; Song, D. UAV-based chlorophyll content estimation by evaluating vegetation index responses under different crop coverages. *Comput. Electron. Agric.* **2022**, *196*, 106775. [[CrossRef](#)]
16. Johnson, M.D.; Hsieh, W.W.; Cannon, A.J.; Davidson, A.; Bédard, F. Crop yield forecasting on the Canadian Prairies by remotely sensed vegetation indices and machine learning methods. *Agric. For. Meteorol.* **2016**, *218–219*, 74–84. [[CrossRef](#)]
17. Yoshino, K.; Setiawan, Y.; Shima, E. Land Use Analysis using Time Series of Vegetation Index Derived from Satellite Remote Sensing in Brantas River Watershed, East Java, Indonesia. *J. Geomat. Plan.* **2017**, *4*, 109–120. [[CrossRef](#)]
18. Kim, H.; Kim, W.; Kim, S.D. Damage Assessment of Rice Crop after Toluene Exposure Based on the Vegetation Index (VI) and UAV Multispectral Imagery. *Remote Sens.* **2021**, *13*, 25. [[CrossRef](#)]
19. Swaef, T.D.; Maes, W.H.; Aper, J.; Baert, J.; Cougnon, M.; Reheul, D.; Steppe, K.; Roldán-Ruiz, I.; Lootens, P. Applying RGB- and Thermal-Based Vegetation Indices from UAVs for High-Throughput Field Phenotyping of Drought Tolerance in Forage Grasses. *Remote Sens.* **2021**, *13*, 147. [[CrossRef](#)]
20. Das, S.; Christopher, J.; Choudhury, M.R.; Apan, A.; Chapman, S.; Menzies, N.W.; Dang, Y.P. Evaluation of drought tolerance of wheat genotypes in rain-fed sodic soil environments using high-resolution UAV remote sensing techniques. *Biosyst. Eng.* **2022**, *217*, 68–82. [[CrossRef](#)]
21. Fullana-Pericàs, M.; Conesa, M.À.; Gago, J.; Ribas-Carbó, M.; Galmés, J. High-throughput phenotyping of a large tomato collection under water deficit: Combining UAVs' remote sensing with conventional leaf-level physiologic and agronomic measurements. *Agric. Water Manag.* **2022**, *260*, 107283. [[CrossRef](#)]
22. BMKG; BNPB; WFP. *INDONESIA Impact Monitoring of Hydrometeorological Hazards July–September 2020*; A Bulletin from BMKG, BNPB and WFP; Badan Meteorologi, Klimatologi, dan Geofisika, Badan Nasional Penanggulangan Bencana and World Food Programme; BMKG; BNPB: Jakarta, Indonesia; WFP: Rome, Italy, 2020.
23. Kanemasu, E.T. Seasonal Canopy Reflectance Patterns of Wheat, Sorghum, and Soybean. *Remote Sens. Environ.* **1974**, *3*, 43–47. [[CrossRef](#)]
24. Motohka, T.; Nasahara, K.N.; Oguma, H.; Tsuchida, S. Applicability of Green-Red Vegetation Index for Remote Sensing of Vegetation Phenology. *Remote Sens.* **2010**, *2*, 2369–2387. [[CrossRef](#)]
25. Huang, S.; Tang, L.; Hupy, J.P.; Wang, Y.; Shao, G. A commentary review on the use of normalized difference vegetation index (NDVI) in the era of popular remote sensing. *J. For. Res.* **2021**, *32*, 1–6. [[CrossRef](#)]
26. Zhang, Y.; Su, Z.; Shen, W.; Jia, R.; Luan, J. Remote Monitoring of Heading Rice Growing and Nitrogen Content Based on UAV Images. *Int. J. Smart Home* **2016**, *10*, 103–114. [[CrossRef](#)]
27. Jiang, Z.; Huete, A.R.; Didan, K.; Miura, T. Development of a two-band enhanced vegetation index without a blue band. *Remote Sens. Environ.* **2008**, *112*, 3833–3845. [[CrossRef](#)]
28. Maki, M.; Katsura, K.; Oki, K. Comparison of Empirical Regression Models for Estimating LAI of Paddy Rice from Several Vegetation Indices Derived from UAV Images. *J. Remote Sens. Soc. Jpn.* **2016**, *36*, 100–106.
29. Walsh, O.S.; Shafian, S.; Marshall, J.M.; Jackson, C.; McClintick-Chess, J.R.; Blanscet, S.M.; Swoboda, K.; Thompson, C.; Belmont, K.M.; Walsh, W.L. Assessment of UAV Based Vegetation Indices for Nitrogen Concentration Estimation in Spring Wheat. *Adv. Remote Sens.* **2018**, *7*, 71–90. [[CrossRef](#)]
30. Su, T. Efficient paddy field mapping using Landsat-8 imagery and object-based image analysis based on advanced fractal net evolution approach. *GIScience Remote Sens.* **2017**, *54*, 354–380. [[CrossRef](#)]

**Disclaimer/Publisher's Note:** The statements, opinions and data contained in all publications are solely those of the individual author(s) and contributor(s) and not of MDPI and/or the editor(s). MDPI and/or the editor(s) disclaim responsibility for any injury to people or property resulting from any ideas, methods, instructions or products referred to in the content.